



Plan Shape Geomorphology of Alluvial Valley in the Middle-Lower and Deltaic Courses of the Subarnarekha River Basin, India

Subrata Jana and Ashis Kumar Paul

Abstract

The middle-lower and deltaic courses of the Subarnarekha river from Jamsola (upstream) to Chaumukh (mouth) have been considered for the study of plan shape geomorphology partially along the alluvial valley floors between bank margin environment. Geologically and topographically, the depositional environments comprise with Lalgah formation, Sijua formation, Panskura formation, Basudebpur formation, Daintikri formation, and beach ridge chenier formations of fluvial, fluvio-marine and marine depositional processes with the seaward gradient from Jamsola to Chaumukh. Distinctive sub-environments of the upstream fluvial dominance, ancient delta-fan lobe extension, and areas of sea level fluctuations with lower deltaic beach ridge chenier at downstream section are categorized based on the identified assemblages of landforms in the present study. The geospatial

techniques, repeated field observations, Total Station survey and sedimentological analysis of bank margin stratigraphic sections have been considered in the study to explore the spatial diversity of plan shape geomorphology in the different sections of the studied river course. The study reveals that the course of the river sections bears diverse geometry of meander properties with discontinuous straight courses and wider valleys. The section-wise plan shape geomorphological features assemblages of 16 categories in the section of Jamsola–Ragra stretch, 18 categories in Ragra–Dantan stretch, 15 categories in Dantan–Rajghat stretch, and 24 categories in Rajghat–Chaumukh stretch in the form of instream deposition, channel fringe deposition and floodplain deposition. Distinct morphological variations of the three major mid-channel bars at the different channel positions indicate the nature of seasonal hydrodynamics and signatures of catastrophic floods. The layer-wise sedimentological analysis of the younger fill terrace and two mid-channel bars shows the trend of discharge and fluctuating flow regimes in the different flood events of single or multiple years. Identification of palaeo-shorelines, ancient delta-fan lobes and cut and fill terraces along the courses of the river valley highlights the role of dynamic marine, fluvio-marine and fluvial environments in the region.

S. Jana (✉)
Department of Geography, Belda College, Belda,
Paschim Medinipur, India

A. K. Paul
Department of Geography and Environment
Management, Vidyasagar University, Midnapore,
India

Keywords

River valley geomorphology · Geological formations · Fluvio-marine depositional environments · Seasonal hydrodynamics · Sedimentological analysis

3.1 Introduction

The distinct geomorphological features within a river valley formed in a suitable position, and their shape and size are modified based on the interacting processes of fluvial hydraulics and sediment loads within a river valley region (Bentham et al. 1993; Ashworth et al. 2000; Sarma 2005; Corenblit et al. 2007; Ventra and Clarke 2018). The existing characteristics of channel geometry also control the dimensions of the geomorphological features (Abrahams 1984; Wharton 1995; Sofia 2020). The diversified river valley geomorphological features form in the longitudinal and transverse section in the different stretches of a river basin (Khan et al. 2018). The types and dimensions of landforms in the hilly or upper catchment areas are far different from the middle and lower catchment areas. Also, the landform types differ according to the lithological features and sedimentary nature (Jana and Paul 2019). In the tropical region, the middle and middle-lower reaches of a river valley are dominated by soft sedimentary deposits (Fryirs and Brierley 2012; Jana 2019). In these reaches, landforms formed under the unidirectional flow, which enhanced during the summer monsoon flood season (Jana and Paul 2018). However, the landforms in the extreme lower reaches or deltaic areas are dominated by silt and clay types of material deposited by the bidirectional tidal flow (Jana and Paul 2018). At the overbank flow regimes, the sediment loaded flood water can reach up to the valley ends. The new or already existed geomorphological features formed or restructured, depending on the flow energy level, the volume of water and sediment and inundation intensities (Gilvear 1999; Fryirs and Brierley 2012). Concurrently, in the instream section, the geomorphic units also

evolved according to the erosional and depositional nature of sedimentary environments (Leopold et al. 1992). Therefore, to some extent, landform modifications are related to every flood event. Moreover, anthropogenic activities play a significant role in geomorphic alterations within riparian areas (Best 2019).

The identification and demarcation of different instream geomorphic units are a difficult task for their ever-dynamic nature in connection with the seasonal fluctuation of the flow regime (Fryirs and Brierley 2012; Roy and Sahu 2018; Sofia 2020). The floodplain geomorphological features are relatively less altered by the flow regime, although, it modified by the anthropogenic activities (Poff et al. 1997; Wu et al. 2008). Despite the dynamic nature and anthropogenic alterations, the distinctive geomorphic units have well preserved in the different extents of the river valley (Bisson et al. 2017). Those landform units can be identified through the analysis of sedimentary environments, terrain diversities, geometric properties and the presence of soil, vegetation and moisture contents in the different landforms. In this concern, field observations and surveying are the prime tasks coupled with satellite image analysis.

In the present study area of the middle-lower and deltaic courses of the Subarnarekha river valley, lots of works have been done regarding the geological and geomorphological study in the different area specific aspects (Niyogi 1975; Bhattacharya and Misra 1984; Paul 2002; Jana and Paul 2014, 2018, 2019, 2020; Jana et al. 2014; Paul and Kamila 2016; Guha and Patel 2017), morphometric analysis and landforms (Ilahi and Dutta 2016), hydrological aspects (Dandapat and Panda 2013; Samanta et al. 2018) and river bank erosion rate and its prediction (Jana 2019). But, most of these works have been done to a discrete extent, which mainly concentrated in the deltaic areas. Although, some studies have been done considering the entire basin area (Ilahi and Dutta 2016; Guha and Patel 2017), these works did not consider the detailed geomorphological features. The entire middle-lower and deltaic courses are yet not considered

in a uniform aspect for geomorphological analysis. Therefore, the present study aims to assess the distinct geomorphological features at different spatial extents (along and across the valley) of the middle-lower and deltaic courses of the Subarnarekha basin based on the sedimentological and hydrological analysis coupled with field investigations in the different periods.

3.2 Materials and Methods

3.2.1 Study Area

The present study has been carried out in the middle-lower and deltaic courses of the Subarnarekha river valley, extended from the Jamsola (upstream) to Chaumukh (confluence in the Bay of Bengal) (Fig. 3.1). The study area boundary has been selected based on the extent of lateritic cliffs on both sides of the river valley in the middle-lower course (Fig. 3.1). However, in the deltaplain, about 10 km extents on both sides have been considered as the boundary of the study area. The selected area has been extended between 21°32'34.84"N to 22°19'18.48"N and 86°43'21.14"E to 87°28'33.78"E coordinates. The alluvium deposited area has been selected as the study area boundary (Fig. 3.2). However, some patches of laterite and gravel dominated areas have also included within the study area (Fig. 3.2) as it was considered based on the contour values.

Geologically, the selected area was formed during the Late Pleistocene to Late Holocene period comprising the Sijua formation, Panskura formation, Basudebpur formation, Daintikri formation and sand dune and beach formations (Fig. 3.2). The Tertiary gravel bed of Dhalbhum formation and Late Pleistocene laterite surface of Lalgargh formation exists in the extreme boundary extents of the study area (Fig. 3.2) (GSI 1998). The extensive floodplain and valley are observed in the left side (east) of the present river course in comparison with the valley on the right side (west) of the river, particularly within the Jamsola and Rajghat stretch. The present river course is flowing in different directions following the

valley slope i.e. west to east (Jamsola to Ragra), north-west to south-east (Ragra to Dantan), north-east to south-west (Dantan to Rajghat), and again it flows from north-west to south-east direction (Rajghat to Chaumukh) before conflux to the Bay of Bengal. Also, the different landform terraces of cut and fill valley and deltaplain (Fig. 3.3) virtually coexists with the distinctive flow directions. The unidirectional river flow is observed up to Baliapal (from upstream) section, which is dominated during the summer monsoonal flood (Jana, 219). However, the downstream section of Baliapal (recent deltaplain) is dominated by the diurnal bidirectional tidal flow with about 2.31 m mean annual range.

3.2.2 Database and Data Processing

In this study, the Geological Quadrangle Map (GQM) has been collected from the open sources of the Geological Survey of India portal (GSI 1998) to comprehend the lithological formations of the area. The 30 m resolution Shuttle Radar Topography Mission (SRTM) images (coordinates: 21/87, 22/86 and 22/87; acquisition date: 11th February 2000) and Landsat 8 OLI image (path/row: 139/45; acquisition date: 27th February 2015) have been collected from the United States Geological Survey (USGS) based data portal (EarthExplorer). All the maps and images have been re-projected and resampled in the Universal Transverse Mercator (UTM) projection concerning the 45 N zone and World Geodetic Survey 1984 (WGS84) datum. The images have also been co-registered (Beuchle et al. 2015) with < 0.5 pixel accuracy of Root Mean Square Error (RMSE). The atmospheric noise effect has been rectified using the Fast line-of-sight Atmospheric Analysis of Spectral Hypercubes (FLAASH) model followed by Jia et al. (2014). The landuse and landcover (LULC) classification have been done considering the corrected Landsat image using the maximum likelihood and support vector machine (SVM) classifiers models in the ENVI 5.1 software (Foody et al. 1992; Jia et al. 2011; Pal and Foody 2012). The diversified soil, vegetation and water bodies (moist areas)

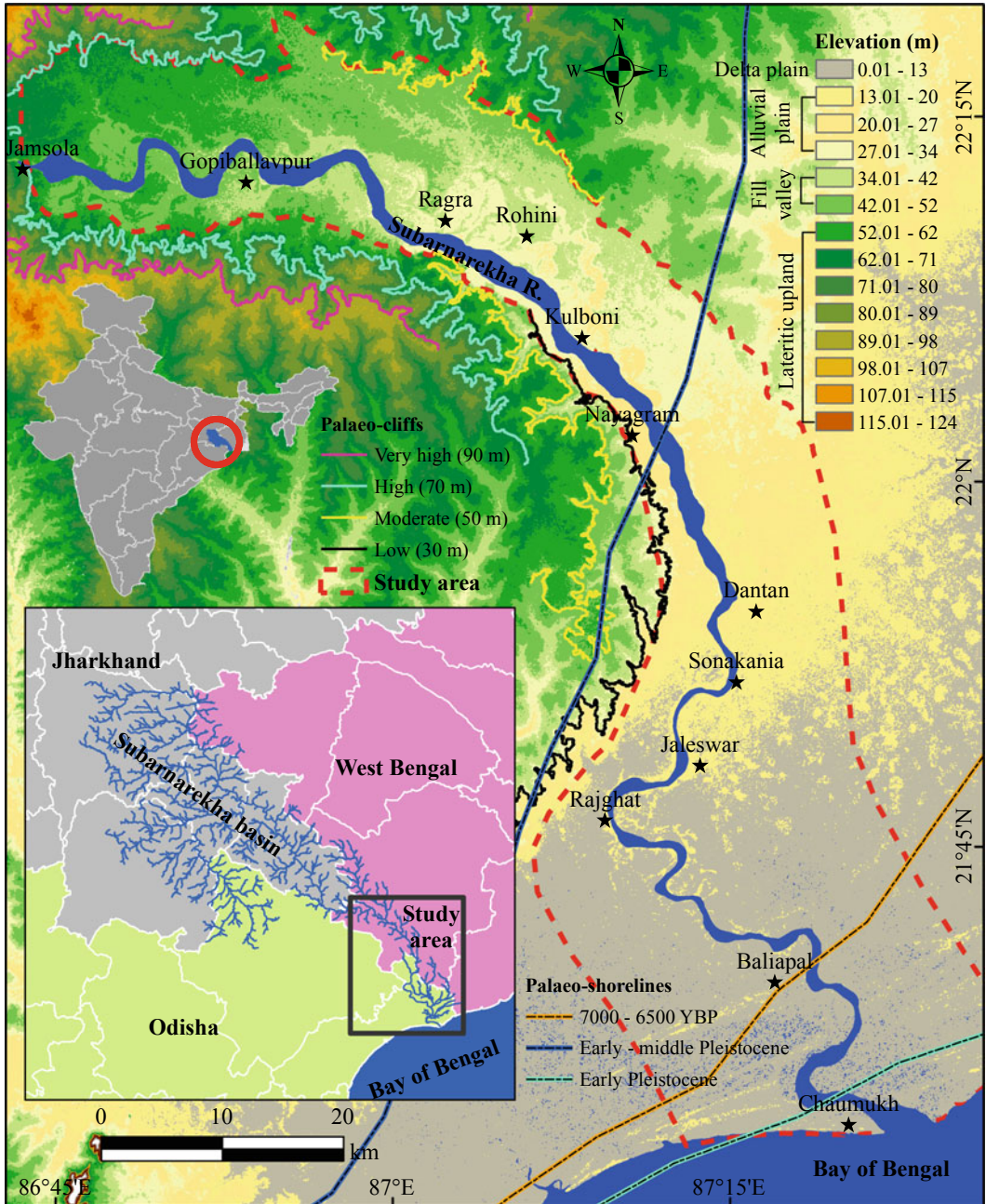


Fig. 3.1 Regional settings of the study area within the fill valley terrace in the middle-lower course and deltaplain of the Subarnarekha river basin

have been identified based on the classified image (Bishop et al. 2012). The elevation data have randomly been taken from ~10,000 locations of different geomorphic units using the

DGPS (Differential Global Positioning Systems). Considering the earth as an ellipsoid surface coupled with the WGS84 datum and Earth Gravity Model 1996 (EGM96) the DGPS is

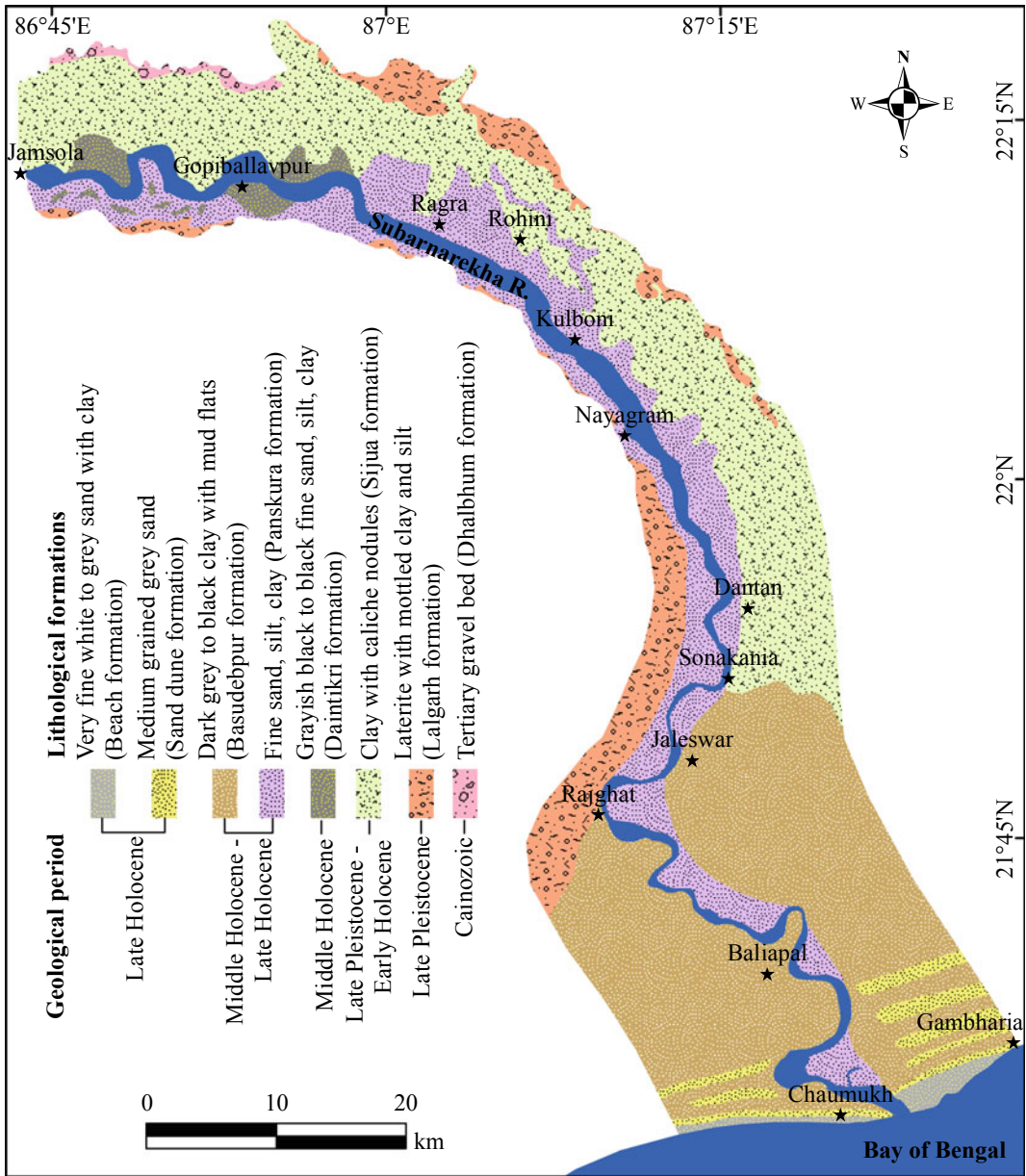


Fig. 3.2 Geological setting of the study area exhibits age-wise different lithological formations

performing. Therefore, the extracted DGPS-based data (elevation) converted into equipotential geoidal surface corresponding to the mean sea level (MSL) as a local vertical datum (Pavlis et al. 2012; Patel et al. 2016). Moreover, the Total Station (TS) survey was conducted during February–April 2015 in the distinct geomorphic units of the river bed, mid-channel bar, natural

levees (older and younger), palaeo-courses and oxbow lake areas. Elevation data of ~1500 points were taken from each site at ~10 m of spatial interval (depending on the elevation differences). The SRTM images have been merged (mosaic) and resampled into 10 m resolution after sub-pixel analysis (Mokarrama and Hojati 2018). The vertical accuracy of the resampled

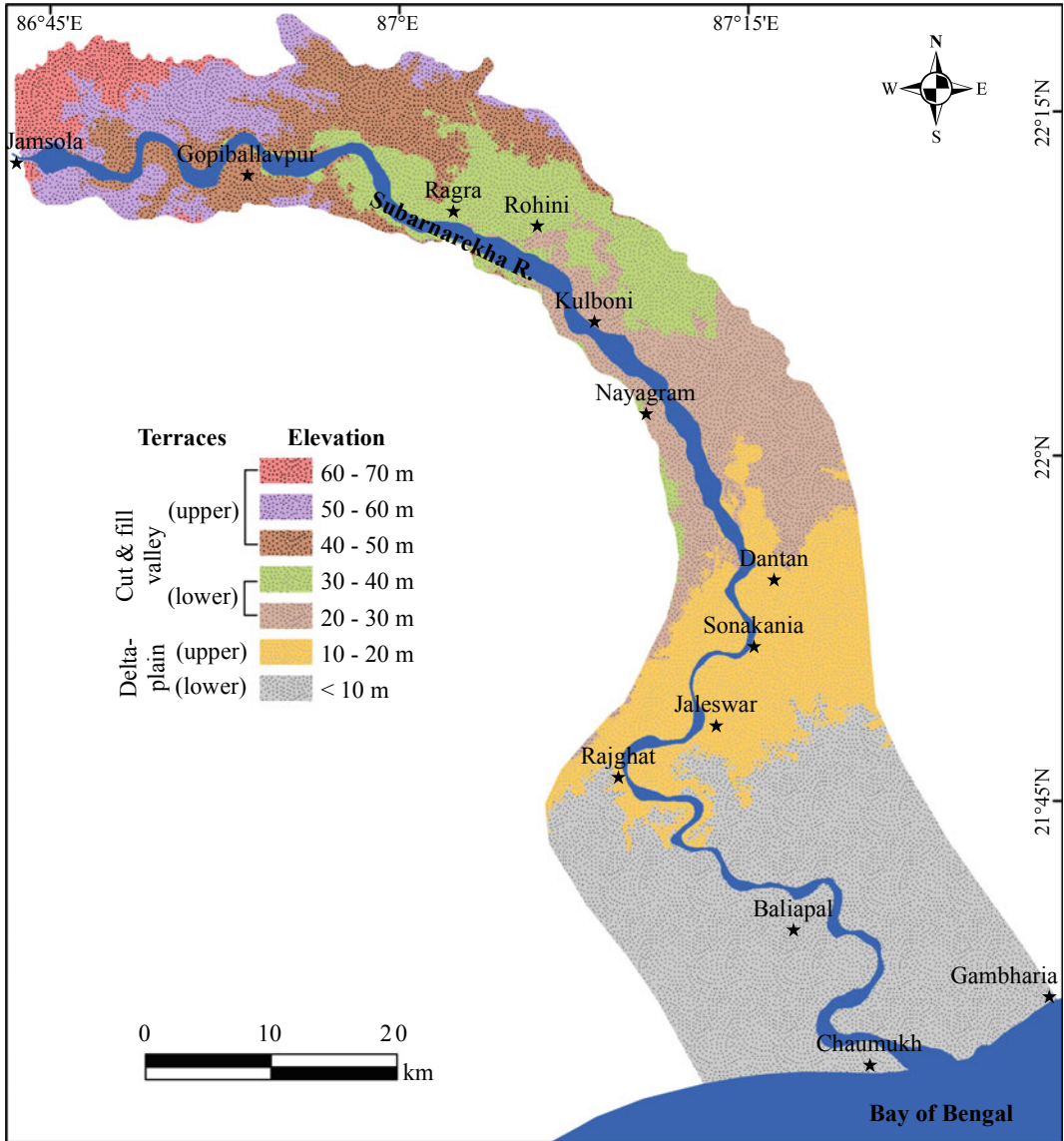


Fig. 3.3 Diversified elevation zones and landform terraces of the study area

SRTM data has been validated with DGPS-based elevations, which reveals the ± 0.15 m RMSE. Moreover, the DGPS and TS survey-based elevation data have been converted into raster data (with 10 m resolution) employing the Inverse Distance Weighting (IDW) interpolation method (Patel et al. 2016), which has been superimposed

on the resampled SRTM data. Finally, the 10 m spatial resolution raster Digital Elevation Model (DEM) has been primed from the assembled dataset. The multi-temporal Google Earth images have also been used for the extraction and validation of different geomorphic landforms.

3.2.3 Extraction of Landform Terraces and Morphological Features

The different landform terraces (cut and fill valley and delta plain) have been demarcated based on the extracted contours (10 m interval) from the finally primed high-resolution (10 m) DEM (Fig. 3.3). Only the extended contour lines have been selected for the demarcation and mapping of different terraces. The fragmented and patchy contours zones have been ignored for the distinctive terrace mapping. The upper and lower terraces of cut and fill valley and delta plain have been discriminated based on the elevation differences. Altogether 44 types of morphological features have been identified applying the DEM-based elevation differences, LULC classification-based soil, vegetation and water (moist) patches, Google Earth images, nature of sediment deposits and field observations. The textural variations of deposited sediments, erosional and depositional signatures, inundation level and periods have been also considered during morphological features identification. The plan shape morphological features of the entire study area have been segmented in four different zones considering the diversified river flow directions coupled with the slope and elevation differences of the terraces.

3.2.4 Geometrical Analysis

The geometrical properties i.e. channel width (w) at bankfull stage and lean-phase, depth of channel (d), width-depth ratio (w/d), meander length (ℓ), meander height (h), radius of curvature (r) of meander and meander arc-length (R_c) have been estimated followed by the Williams (1986), Islam and Guchhait (2017), and Jana (2019) for the sectional river stretches of Jamsola–Ragra, Ragra–Dantan, Dantan–Rajghat, and Rajghat–Chaumukh sections as well as for the entire studied river stretch. The channel width at lean-phase has been estimated based on the Landsat image of 2015. During the extreme flood events

(bank full periods) the cloud free image was not freely available. Therefore, the channel width at bankfull stage was estimated from the on field survey during July–September, 2015 in the different sectional reaches of the river. The other meander properties have been estimated from the 2015 image using the ArcGIS 10.1 software after digitizing the respective banklines and channel middle positions (Jana 2019).

3.2.5 Sedimentological Analysis

Sediment samples have been collected from the apparent lithostratigraphic units of the different landforms in the upper and lower river courses. On 15th March 2015, twelve sediment samples have been collected from the equivalent layers of the excavated profiles in the scrub dominated younger fill terrace (S1) at Dharmapur and older mid-channel bar (S2) at Nayabasan. Moreover, six different sediment samples have been collected (on 26th September 2015) from each of the layers of the mid-channel bar (S3) at Saherbazar near Jaleswar. All three profiles have been excavated up to the exposed layer corresponding to the river bed. The collected sediment sample has been processed and analyzed to discriminate the textural variation of the particles using sieving and pipette methods. The percentage distributions of sediment grain-size have been further analyzed employing the GRADISTAT statistical programme (Blott and Pye 2001) to understand the nature of fluvial environments during sediment deposition in the respective layers.

3.3 Results and Discussion

3.3.1 Fluvio-Marine Environments and Landform Terraces

The cut and fill valley terraces (Fig. 3.3) have been formed and modified with due effects from the fluvio-marine environments during the Early Pleistocene to Holocene period (Fig. 3.2). Initially, the marine process was in action around the lower cut and fill valley terrace (Fig. 3.3)

when the shoreline was parallel to the laterite surface during the Early–Middle Pleistocene period (Fig. 3.1) (Banerjee and Sen 1987, 1988; Jana and Paul 2020). During this period, the laterite cliffs were formed with the relatively fluctuating sea level and associated land erosion by sea waves (Niyogi 1975). The tide-water entered into the future interior areas of the river valley and enhanced the retreating rate of laterite layers progressively towards the land. Moreover, the fluvial action was more active during the Late Pleistocene ice melting in the Bengal Basin area (Ghosh and Guchhait 2020). Therefore, the combined erosional effects of the fluvio-marine processes were responsible for the formation of the extensive valley on both sides of the present river course. However, the four different cliffs at various elevations (Fig. 3.1) have been modified by the headward erosion along the tributaries on both sides of the valley in the Holocene period. The marine regression phase was started and the shoreline was aligned at the Baliapal section during 7000–6500 years before present (YBP) (Banerjee and Sen 1987, 1988; Jana and Paul 2020) almost parallel to the present shoreline (Fig. 3.1). Therefore, the Nayagram–Baliapal stretch was dominated by the fluvio-marine transitional environment during the middle Pleistocene to 6500 YBP (Jana and Paul 2020). Moreover, the existence of five successive chenier dune ridges and swales between the Contai and Digha-Talsari coastal stretch reveals the continuous regression phase with a limited period of stillstand phases during 6,000–5,000 YBP, 4,700–4,000 YBP, 3,500–3,000 YBP, 2,500–1,100 YBP, and 600–500 YBP (Goswami 1997, 1999; Jana and Paul 2020).

The extended valley has been filled up by the river carried sediments drained from the upper catchment areas and the nearby laterite uplands during the Late Pleistocene to middle Holocene periods (Jana and Paul 2019, 2020). These cut and fill valley terraces (Fig. 3.3) have remained under the Sijua formation, Panskura formation and Daintikri formations composed with the fine sand, silt and clay type of materials (Fig. 3.2).

The river was flowing nearer the laterite surface on the left side of the valley in the past. Recently, the river is flowing through the relatively meandering path within the upper terrace (40–70 m elevation) maintaining the gentle surface gradient. The eroded materials from the retreated lateritic cliffs have been deposited in this area, which is responsible for the higher elevation. The river flows in the straight course within the lower terrace (20–40 m elevation), and the relatively higher gradient is perceived the lower terrace in compared to the upper terrace. The deposited materials in the lower terrace have been redistributed and somehow transported towards the downstream section under the dominance of the fluvial environment. These sediments were deposited (as a delta-fan) in the upper delta plain during the accelerated rate of marine regression at the later phase of the Middle Pleistocene period (Jana and Paul 2020). Therefore, among the two cut and fill valley terraces, the lower terrace is more extended than the upper terrace, although, the higher elevation differences are experienced in the upper terrace area (Fig. 3.3). Initially, both delta plain was formed as the submerged delta-fan lobes when the corresponding shorelines remained in the landward extents. However, the submerged delta-fans were emerged due to continuous sediment deposition in the shallow marine environments coupled with the marine regression effects since the middle Pleistocene period (Paul 2002). The initially deposited deltaic sediment of the upper delta plain has been overlain with the sedimentary deposits of the Sijua and Panskura formations, whereas, most of the lower delta plain area has remained under the Basudebpur formation (Figs. 3.2 and 3.3). The dominant meandering channel pattern was formed with due effects from the marine regression and short-term stillstand phases within the delta plain (Paul 2002). Recently, the entire upper delta plain is controlled by the unidirectional flow, which is dominating during the summer monsoon period, whereas, the tide-water (marine environment) still dominated up to the middle section of the lower delta plain (Baliapal).

3.3.2 Geometrical Diversity of River Course

Geometrical properties of the river course have been estimated (Jana 2019) considering the four different river stretches and the overall river course within the study area (Table 3.1). In the Jamsola–Ragra section, the 1032 m average channel width in the bankfull stage is reduced up to 265 m in the lean-phase of active channel flow. The instream geometrical properties are also changed depending on such seasonal fluctuation of river discharge. This meandering course is characterized by the sinuosity index (SI) of 1.37 and the average width/depth ratio (w/d) of 122. The geometrical properties of meander i.e. average length (ℓ), height (h), radius of curvature (r) and arc-length (R_c) have resulted as 7513 m, 2898 m, 1624 m and 10,166 m, respectively. The river course become straightens within the Ragra–Dantan section with resultant SI of 1.07. Therefore, the meander geometrical properties have not been estimated in this section. The estimated average channel width (1512 m) in the bankfull stage is greater than the upper stretch. However, the width of the active channel flow (270 m) in the lean-phase is almost similar to the upper section. The highest average w/d (231) has been estimated in this river stretch among the four zones. At the downstream section (Dantan–Rajghat), again the river course becomes meandering with SI of 1.34. The channel width is decreased up to 598 m in the bankfull stage, and the active channel flow is observed only within 200 m width in the lean-phase. In this section, the lowest w/d (100) is observed among the four stretches. The average estimated meander geometrical properties of ℓ (7207 m), h (3240), r (1355 m) and R_c (9955 m) are somehow minimized in comparison to the Jamsola–Ragra stretch. The prominent meandering channel pattern (SI = 1.54) is observed in the deltaic course in-between the Rajghat–Chaumukh stretch. The average channel width is also wider than the preceding stretch (Dantan–Rajghat), which is \sim 879 m during the peak monsoonal discharge coupled with the extreme high-tide condition. During the lean-phase of monsoon and low-tide

conditions, the active flow is concentrated within 500 m width. In this fluctuating hydrodynamic condition, the average w/d is recorded as 208. The average values of meander geometrical properties are estimated as ℓ (5539 m), h (2410 m), r (1055 m) and R_c (8136 m).

3.3.3 Plan Shape Geomorphology and Depositional Environments

The river valley geomorphological features have been classified into three parts i.e. in the instream, at the fringe of river course and within the floodplain. Moreover, the regional diversities in the plan shape geomorphological features have been broadly categorized in four distinct zones of upper and lower terraces in the cut and fill valley and deltaplain terraces. The depositional environments have been assessed by the repeated field observations of the distinct geomorphic units in different seasons coupled with sedimentological characteristics. Within the selected study area, 22 types of geomorphic units with their subdivisions have been demarcated and analyzed considering the process of formation and present status (Table 3.2).

3.3.3.1 Geomorphological Features in the Upper Cut and Fill Valley Terrace

The sixteen major geomorphological features have been demarcated within the upper cut and fill valley terrace extended from Jamsola to Ragra stretch (Fig. 3.4). Four major coupled with thirteen micro-level diversified geomorphological features have been observed in the instream section. Seven major geomorphic units have been observed at the fringe of the river course, whereas, five features have remained in the floodplain areas (Fig. 3.4). The micro-level diversities of the mid-channel bars and fill terraces have been identified within this stretch.

The active channel flow, recent deposits of sand bodies in the channel bed and mid-channel bar, seasonal and matured mid-channel bars have been observed in the instream position (Fig. 3.4).

Table 3.1 Geometrical properties of river course in the different stretches of the Subamarekha river

| Geometrical properties | Jamsola–Ragra | | | Ragra–Dantan | | | Dantan–Rajghat | | | Rajghat–Chaumukh | | | Overall | | |
|---|---------------|------|--------|--------------|------|------|----------------|------|------|------------------|------|------|---------|------|------|
| | Max | Min | Avg | Max | Min | Avg | Max | Min | Avg | Max | Min | Avg | Max | Min | Avg |
| Channel width (w) at bankfull stage (m) | 2384 | 160 | 1032 | 2087 | 870 | 1512 | 1051 | 260 | 598 | 2424 | 308 | 879 | 2424 | 160 | 1006 |
| Channel width at lean-phase (m) | 450 | 68 | 265 | 450 | 152 | 270 | 272 | 141 | 200 | 2424 | 175 | 500 | 2424 | 68 | 317 |
| Depth (d) of channel (m) | 15.54 | 5.18 | 8.84 | 12.80 | 3.35 | 7.24 | 9.14 | 3.05 | 5.79 | 7.92 | 3.05 | 5.12 | 15.54 | 3.05 | 6.75 |
| Width-depth ratio (w/d) | 222 | 58 | 122 | 405 | 144 | 231 | 144 | 63 | 100 | 795 | 61 | 208 | 795 | 58 | 170 |
| Meander length (m) | 10,679 | 5197 | 7513 | – | – | – | 9732 | 5857 | 7207 | 8423 | 3717 | 5539 | 10,679 | 3717 | 6532 |
| Meander height (m) | 3404 | 2008 | 2898 | – | – | – | 5481 | 1469 | 3240 | 3610 | 840 | 2410 | 5481 | 840 | 2760 |
| Radius of curvature of meander (m) | 4046 | 589 | 1624 | – | – | – | 2455 | 569 | 1355 | 2671 | 202 | 1055 | 4046 | 202 | 1296 |
| Meander arc length (m) | 12,116 | 8426 | 10,166 | – | – | – | 14,159 | 6730 | 9955 | 12,953 | 4357 | 8137 | 14,159 | 4357 | 9183 |

Note The ‘–’ in the Ragra–Dantan stretch reveals that the meander geometrical properties did not estimated in the relatively straight river course

Table 3.2 Different morphological features of the study areas

| Positions | Morphological features | Formation process | Field description |
|------------------------|---|---|---|
| Instream | Active channel flow | Channel flow path throughout the year | Seasonal changes in flow pattern and it depends on the discharge, sediment load and sediment distribution |
| | Channel bed sand bodies (recent deposits) | Long-term flood deposits | Exists in same position and or change their position, shape and size depending on the consecutive flood nature |
| | Mid-channel bar (seasonal) | Resent fluvial deposits | Position, shape and size are changed depending on the seasonal fluctuation of hydraulic and sedimentation nature |
| | Mid-channel bar (stable) | Long-term flood deposits | Erosive marginal part, and nearly stable and vegetated surface platform |
| | Tidal shoal | Tidal deposits at turbidity maximum zone | Elongated shaped, grass and mangrove dominated |
| Fringe of river course | Incipient crevasse channel | Development of a narrow channel after breaching the bar during extreme flood | Narrow channel bifurcates the mid-channel bar deposits |
| | Chute flow | Secondary flow during high flood events | Sluggish palaeo-flow path and only active flow observed during extreme flood event |
| | Chute bar | Degradation of mid-channel bar by storm flood | Degraded and almost abolished |
| | Dead slough | Shifting of active flow path from the bank margin to channel middle position | Sluggish or ponding flow path at the margin of river bed |
| | Sand splays | Sand deposition during storm flood | Exists in the same location and utilized for cultivable land after removal of sand from the top layer |
| | Fill terrace (younger) | Sediment deposits (recent) during flood at the position of earlier cut terrace | Exists in the same position (channel margin) and or changing its position, shape and size depending on sedimentation nature |
| | Fill terrace (older) | Sediment deposits (earlier) during flood at the position of earlier cut terrace of active flow path | Exists at the channel margin position |
| In the floodplain | Backswamp | Diversion of natural river flow after embankment construction | Depression areas at the palaeo-flow path of river |
| | Marshy land | Natural depression areas of the floodplain, mainly form in the swale topographic condition | Initially remained as marshy land and habitat for natural aquatic species and recently altered into aquaculture farm |
| | Oxbow lake | Isolated parts of palaeo-meander course formed after meander neck-cut | |
| | Natural levee (younger) | Sedimentation over marginal areas of recent river course during high flood discharge | Almost entirely occupied by dwellers for settlement and agricultural purpose |
| | Natural levee (older) | | |

(continued)

Table 3.2 (continued)

| Positions | Morphological features | Formation process | Field description |
|-----------|-----------------------------------|---|--|
| | | Sediment deposition in the marginal areas of the palaeo-river course during peak flood discharge | |
| | Meander scrolls (palaeo-channels) | Imprint of the migration of palaeo-river courses | Mostly converted into the agricultural land and fisheries by human activities |
| | Floodplain | Overbank sediment deposition in the extensive low-lying areas on the both sides of the river course | Intensively used for agricultural activities and human settlement |
| | Dune ridge | Sand deposits over the beach ridge surface by Aeolian process | Parallel elevated dunes occupied by settlement with orchards and some natural vegetation |
| | Swale | Tidal mud deposits at the interdune depression areas | Exists as natural wetlands and mostly altered into cultivated areas |
| | Mudflat | Tidal flat deposits over the shallow marine buffer zone | Dominated by the mangroves and salt marshes |

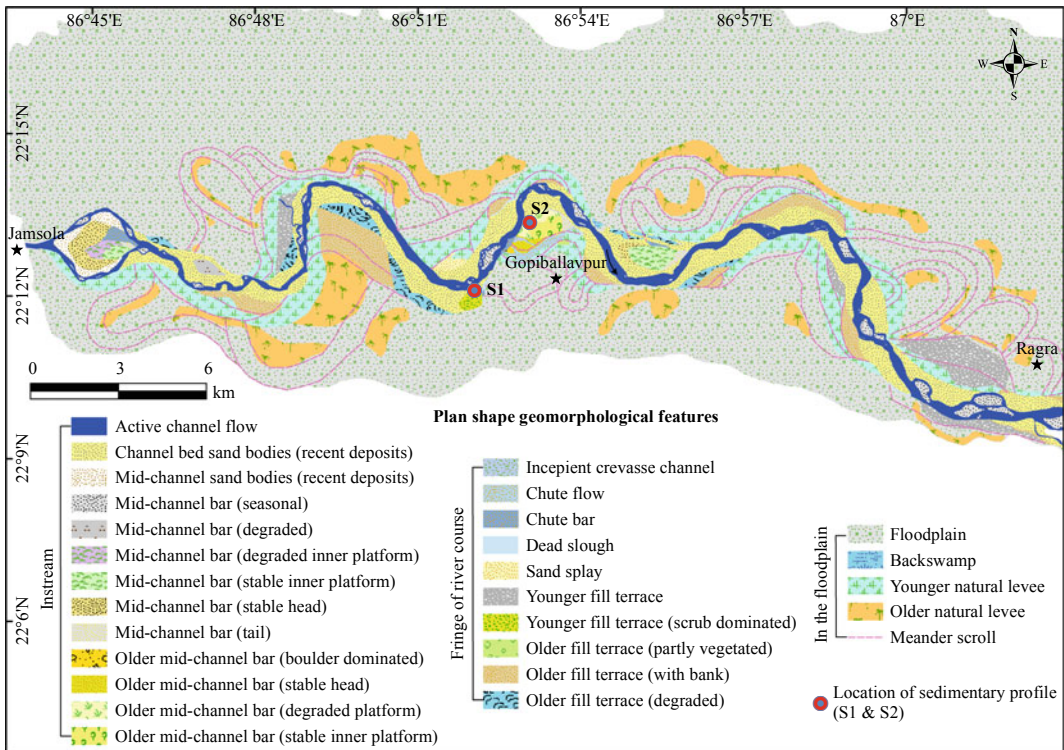


Fig. 3.4 Plan shape geomorphological features of the upper cut and fill valley terrace within the Jamsola–Ragra stretch

Three mid-channel bars have been observed within this river stretch. Among these, one is located in the channel middle position (at Dipapal), and the other two in the channel fringes at Nayabasan (right bank side) and Hatipata (left bank side). Initially, the channel fringe mid-channel bars had remained in the channel middle positions. But, due to the channel shifting on the opposite direction (Jana 2019), these bars have remained in the channel fringe positions. However, these two bars have been surrounded by the river flow during the summer monsoon flood events. The channel bed sand bodies have been deposited on both sides of the channel active flow (during lean-phase). The spatial extents of the sand sheets have been changed depending on the meandering nature of the flow path, hydraulic behaviour of flow during flood events and river bed elevation differences. The seasonal mid-channel bars have been observed in the middle positions of the active flow. These bars have been noticed in the lean-phase of monsoon with due effects from the low magnitude river flow regime. The seasonal mid-channel bars have remained in pseudo nature with their ever-changing positions and extents.

At the fringe of the river course, the incipient crevasse channel, chute flow and bars, dead slough, sand splay, younger and older fill terraces have been found in the Jamsola–Ragra stretch (Fig. 3.4). The incipient crevasse channel has been formed in the Nayabasan bar due to sediment breaching during the extreme flood event (Table 3.2). The chute flow has also been observed in the extreme right bank position of the Nayabasan bar. Initially, this chute flow path remained as the active channel flow path. However, this flow path became gradually inactive with the leftward channel shifting (Jana 2019). The chute bars have been observed in the four different positions, three in the marginal positions of mid-channel bars and one in the margin of the scrub dominated younger fill terrace. The dead slough has formed due to the flow path shifting from the bank margin to the channel

middle position and the remnant flow path converted into the sluggish flow path. Such types of micro-geomorphic units have been observed at the five different positions in Jamsola–Ragra stretch (Fig. 3.4). The sand splay has been found in the left bank position, just on the opposite side of scrub dominated younger fill terrace (Fig. 3.4), which has been formed due to the sand deposition at the overbank flow regime during the storm flood events. The younger fill terraces have been formed with recent sediment deposits during the flood events. However, the positions of the fill terraces were remained as the cut terrace in the near past, which were also remained as the active flow path of the earlier river course. The older fill terraces have been formed in the same process likewise the formation process of the younger fill terraces. Only the difference is that the older fill terraces are older and remained far away from the recent river course compared to the younger fill terraces. In this stretch, three types of older fill terraces have been categorized depending on the vegetation significance and degradation level (Fig. 3.4).

In the floodplain areas, the backswamp, younger and older natural levees, meander scrolls coupled with floodplain have been observed in the different sections away from the river course (Fig. 3.4). The backswamp exists in the backside of the bridge protective embankment structure (left bank) at Gopiballavpur (Jana 2019). The younger levees have been formed due to sediment deposition over the recent channel margin areas. The older levees have situated corresponding to the meander scrolls, which were formed due to the sedimentation in the marginal areas of the palaeo-courses. The overall positions of the meander scrolls in the Jamsola–Ragra stretch reveals that the river course has been migrated on both sides of the recent course. However, the positions of palaeo-cliffs, existing meander scrolls and extents of floodplain in this stretch divulge that the river course has shifted at a large extent towards the right in compared to the leftward shifting.

3.3.3.2 Geomorphological Features in the Lower Cut and Fill Valley Terrace

In the lower cut and fill valley terrace of Ragra–Dantan stretch, similar types of geomorphic features have been observed as mentioned in the Jamsola–Ragra stretch, however, the micro-level diversities have resulted in their forms and characteristics (Fig. 3.5). Two outstanding mid-channel bars have been observed near Rohini and Ragra at the confluence positions of Dulung river with the mainstream of Subarnarekha river (Fig. 3.5). The positional extents of the meander scrolls at the confluence region divulge that this area remained as a depression like area in the past. Another mid-channel bar has been situated at the downstream section of Kulboni and near Nayagram. The mid-channel bar located near Rohini is enough elevated and stable, which is well known as Kodopal. The diversified micro-geomorphic units of chute flow with chute bars, dead slough and bar tails have been observed in the Kodopal. The active river flow has dispersed along the wide channel bed in the relatively straight river course. Therefore, a large number of seasonal mid-channel bars are present that river stretch compared to the other stretches. The extended younger fill terrace on the right side of the recent course reveals that the river is migrated towards the left at most of the positions. However, the position of palaeo-cliffs (Fig. 3.1), meander scrolls and associated older natural levees and extensions of floodplains (Fig. 3.5) demonstrate that the river was flowing with a meandering channel pattern in the past and gradually straightened its course by the rightward shifting. The marshy lands have been formed at the positions of palaeo-courses.

3.3.3.3 Geomorphological Features in the Deltaplain

The meandering course of the upper deltaplain is extended within Dantan–Rajghat stretch. This section is now converted into the ancient deltaplain (Jana and Paul 2019). The minimum numbers of geomorphic units have been observed in this stretch (Fig. 3.6) compared to the other stretches. The younger fill terraces have

remained at the concave meander bends, whereas, the younger natural levees have been extensively situated almost in both sides of the river course. The positions of the meander scrolls reveal that the palaeo-course was relatively straight, which gradually follow the meandering pattern. However, the most complex channel pattern has been observed in the lower deltaplain of the Rajghat–Chaumukh stretch (Fig. 3.7). This river stretch has been associated with the unidirectional and bidirectional flow nature respectively in the upstream and downstream of Baliapal sections. Though, this entire river stretch was tide-dominated during 7000–6500 YBP (Paul 2002; Jana and Paul 2020). Almost similar types of geomorphological features have remained in this stretch (Fig. 3.7) as observed in the earlier stretches (Figs. 3.4, 3.5, and 3.6). However, the mature and immature tidal shoals, oxbow lakes, dune ridge, swale and mudflat are the additional geomorphic features in the lower deltaplain (Fig. 3.7). The tidal shoals have been formed at the turbidity maximum zones in the extremely tide-dominated lower course (Paul and Kamila 2016). The lower elevated immature tidal shoals have been submerged and emerged depending on the tidal range, whereas, the mature shoals have remained emerged and are significantly covered by saltmarsh and mangroves. The linear array of dune ridges have remained coupled with inter-dune swales within the chenier deltaplain. The elongated mudflat has been formed in the modern barrier coast of the Subarnarekha deltaplain (Jana et al. 2014; Jana and Paul 2019). The existence of oxbow lakes in the palaeo-courses reveals that the river course was active in the near past (Jana and Paul 2020). The younger levees and fill terraces have dominated within this entire river stretch. The older natural levees have been mainly found in the upper section (Rajghat–Baliapal), whereas, the older fill terraces in the lower section of Baliapal. The relative positions of the natural levees and fill terraces (younger and older), oxbow lakes and meander scrolls reveal that the river course has been shifted on both sides in the different sections. However, the river was shifted at a larger extent on the leftward (within the Rajghat–

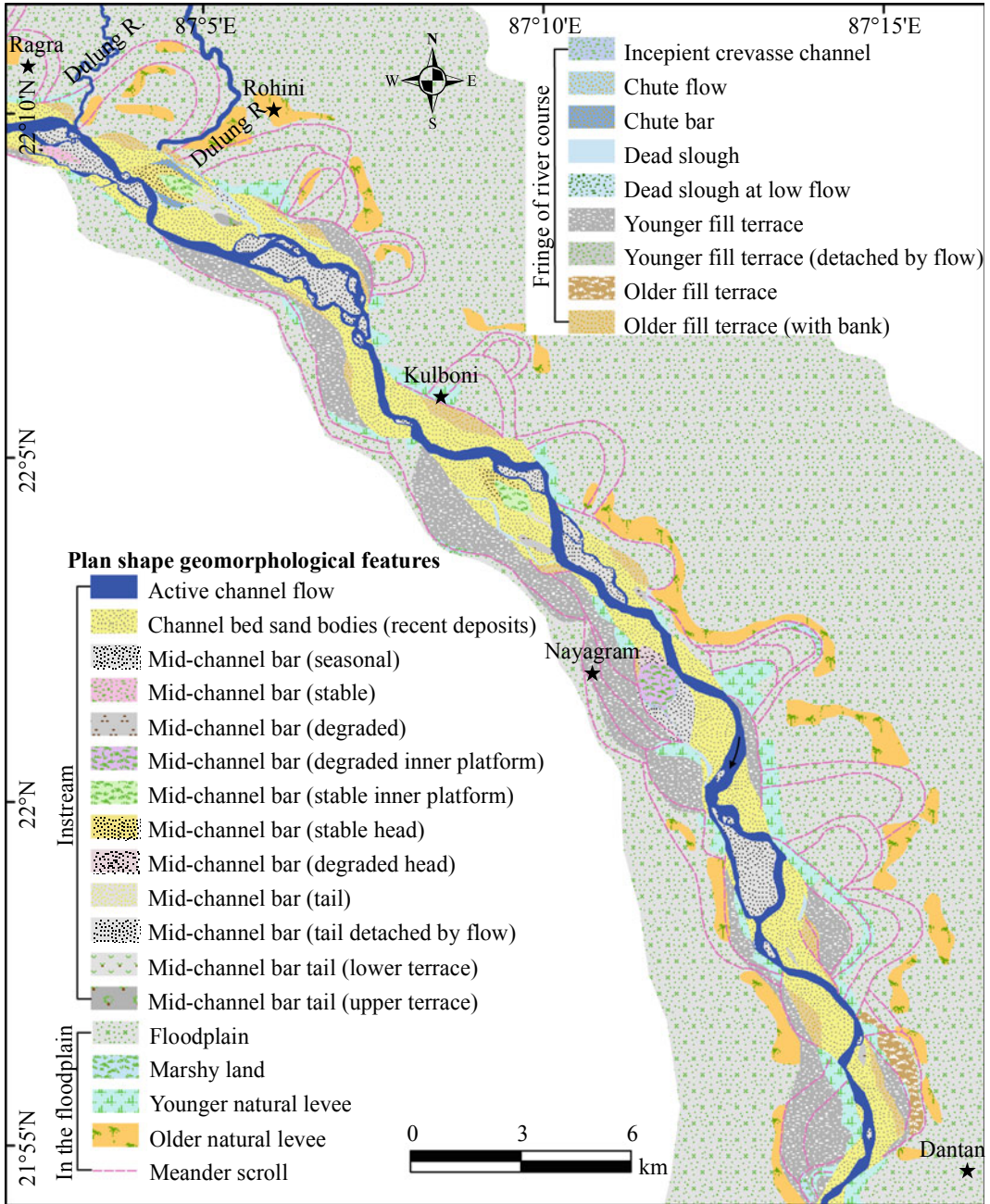


Fig. 3.5 Plan shape geomorphological features of the lower cut and fill valley terrace within the Ragra–Dantan stretch

Baliapal section), both sides at a similar trend (near Baliapal) and rightward (near upstream of Chaumukh) depending on the hydrodynamic nature coupled with the river geometry. Also, the pattern and positions of dune ridges on both sides

of the river course (straight and curved ridge cutting) reveals that initially, the river was flowing in a straight course at the downstream of Baliapal, whereas, it was continuously migrating rightward and ensured the meandering flow path

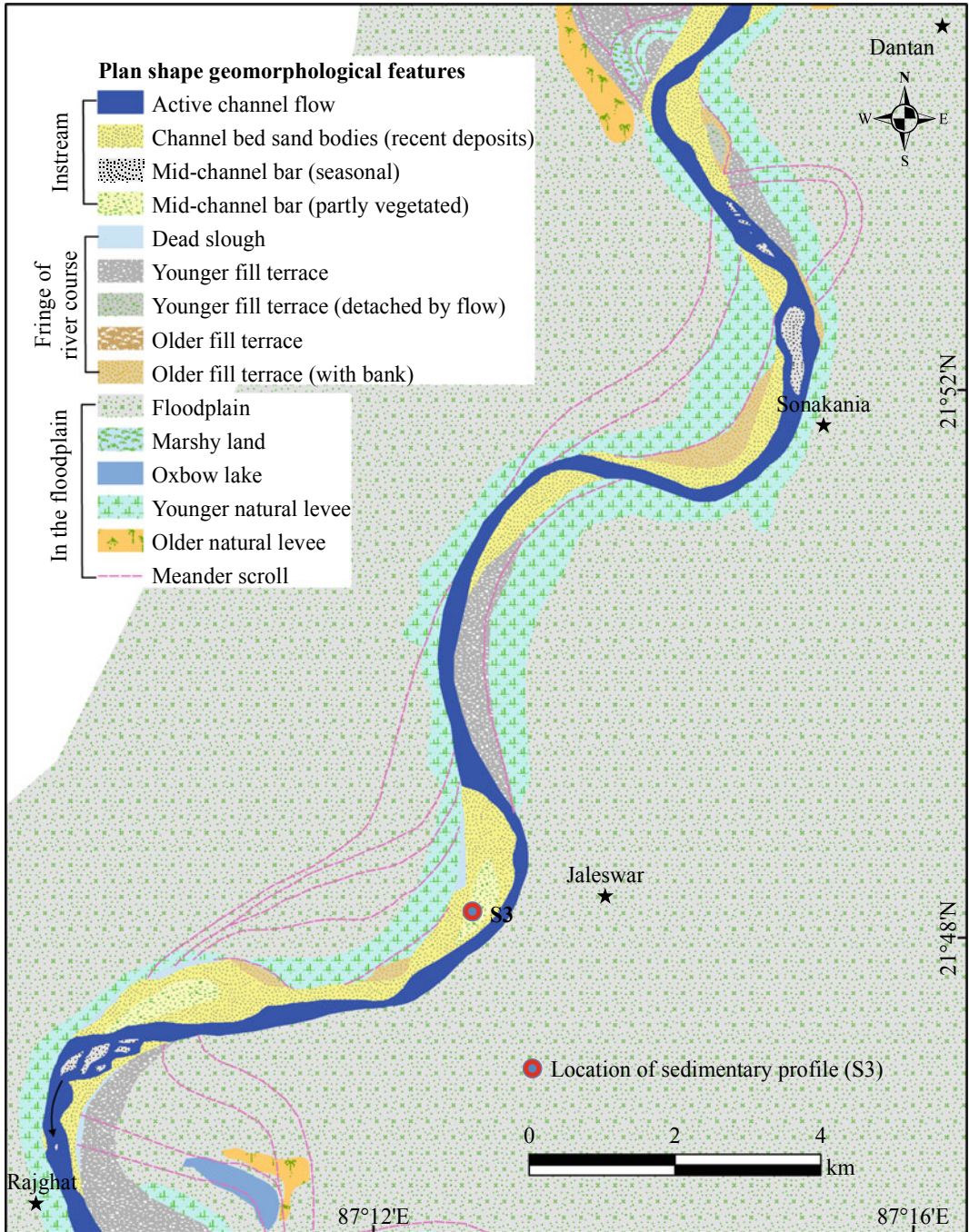


Fig. 3.6 Plan shape geomorphological features of the upper delta plain within the Dantan–Rajghat stretch

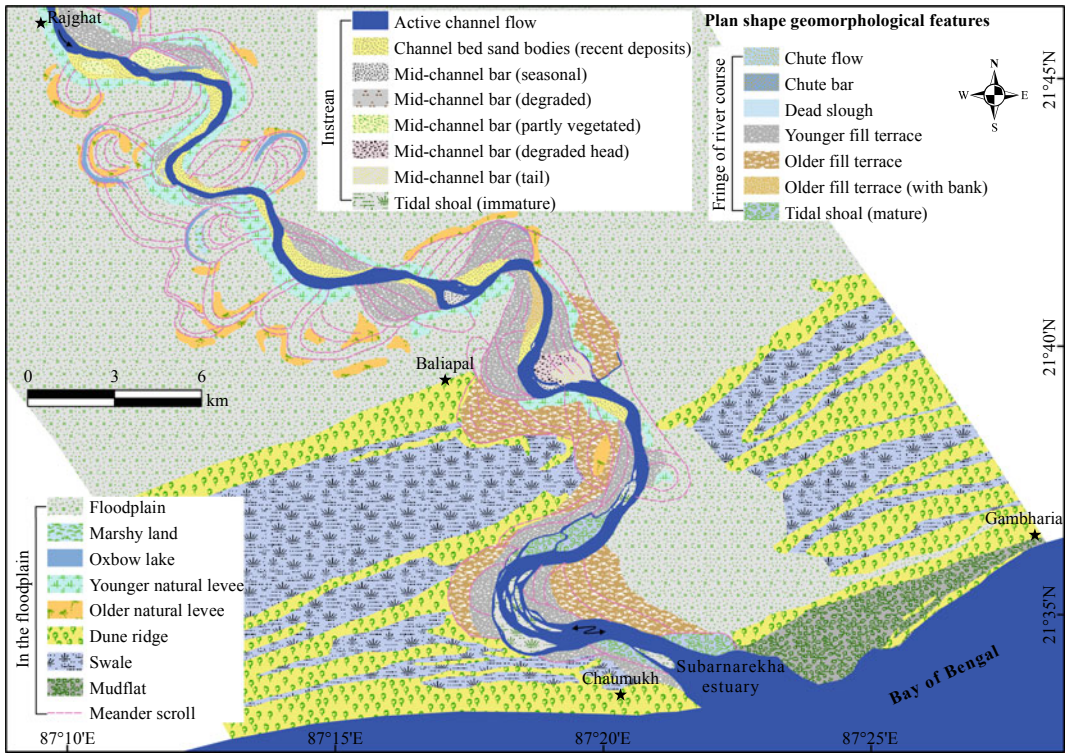


Fig. 3.7 Plan shape geomorphological features of the lower delta plain within the Rajghat–Chaumukh stretch

in the extreme right bank position. However, the existence of fill terraces in both banks coupled with tidal shoals within the present river course reveals that the river width has been shrunk through maintaining the hydrodynamic adjustments associated with the fluctuating sea level.

3.3.4 Morphology of Mid-Channel bar

Just after the Jamsola gorge section, the channel width has increased from 160 m to 2384 m within 2 km river stretch (Figs. 3.4 and 3.8a). The largest (2.38 km²) mid-channel bar (surrounded by the mid-channel sand bodies) has been formed at Dipapal with due effects from the abrupt diminution of hydraulic energy in the extensive river course. However, the entire bar is not in a stable form and it has been categorized in five different platforms (bar head, chute bar, bar tail, degraded inner bar platform and stable bar

platform) depending on the elevation differences and surface expressions of degradation level (Fig. 3.8a). This bar is about 8.5 m elevated from the surrounding river bed. The river flow is bifurcated and it again converged in a single flow in this section. Another significant mid-channel bar (older) has been observed at Nayabasan (right bank side) covering an area of 2.13 km² (Figs. 3.4, and 3.8b). The maximum height of this bar is about 6.75 m in respect to the local river bed. The distinctive geomorphological features of stable inner bar platform, degraded bar platform, stable bar head, chute bar, boulder dominated bar head, bar tail coupled with incipient crevasse channel, dead slough and chute flow path have been found in this section (Fig. 3.8b). The chute flow path initially remained as the main flow path of the active channel. However, recently, flood water can enter within this path only during extreme flood events. During the high magnitude flood events, the river carried boulders have deposited in the

marginal areas of the bar. The chute bar has been formed due to erosion of the mid-channel bar. The inner bar platform has remained in stable condition covered by scattered vegetations, whereas, the outer bar platform has been gradually degraded with due effects from the intensive sand mining from the marginal river bed (Jana 2019). The other mid-channel bar has been situated at Kodopal, which is covered about 1.90 km² area and the upper bar platform remains in 7 m height from the local river bed (Fig. 3.8c). The stable bar head and inner bar platform, bar tail, degraded bar tail (upper and lower terrace), chute bar and dead slough (at low flow) are the micro-level geomorphic features observed in the mid-channel bar section of the Kodopal (Fig. 3.8c). This bar has been formed with due effects from the combined river discharge and sediment load in the straight and wide river course followed by the relatively curved and narrow course in the downstream section. The

voluminous load (water and sediment) might not able to easily drain to the downstream river stretch. Therefore, the lag deposit was responsible for the formation of the mid-channel bar at that position.

3.4 Sedimentary Stratigraphy and Depositional Environments

The sedimentary depositional environments of a landform can be evaluated through the analysis of sedimentary characteristics (Jana and Paul 2020). In this concern, the lithostratigraphic characteristics of three different landforms have been assessed considering the layer-wise diversities of depth (thickness), material types, mean grain-size, mode, sorting, skewness and kurtosis. The sedimentary profile has been excavated up to the 3.58 m.bgl (below ground level) in the channel margin younger fill terrace at Dharmapur

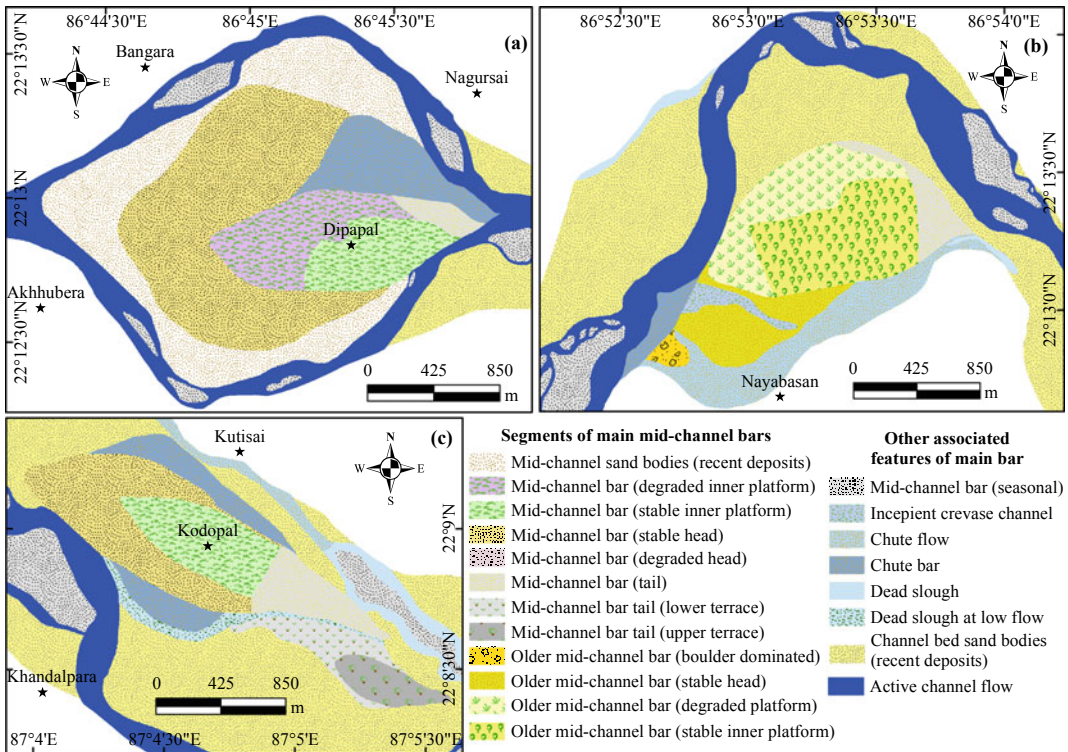


Fig. 3.8 Morphological diversities of the different mid-channel bars situated (a) at Dipapal, in the downstream section of Jamsola, (b) at Nayabasan near Gopiballavpur, and (c) at Kodopal near Rohini

(Fig. 3.4, Table 3.3). The sedimentary profile of the older mid-channel bar has been excavated up to 1.93 m.bgl at Nayabasan (Fig. 3.4 and Table 3.4), whereas, the sedimentary characteristic has been recorded from the 6.11 m thick exposed profile of mid-channel bar at Saherbazar (Fig. 3.6, and Table 3.5). The lithostratigraphic characteristics reveal that the different natures of fluvial environments were effective during the sediment deposition in the distinctive layers (Jana and Paul 2020). Within the three profiles, the material types coupled with the mean grain-size varies from the very coarse sand (with gravels) to clay types, which indicates the very high to very low energy environments. Moreover, the trends of discharge (water and sediment) and energy level coupled with the fluctuating flow regimes have been elucidated through the nature of mode, sorting, skewness and kurtosis (Jana and Paul 2020). The unimodal type of sedimentary characteristics indicates the steady flow of a single flood event, whereas, bimodal nature is characterized by two or more flood events or can be a repetitive fluctuating energy level in a single flood event. The well sorted sedimentary nature reveals the mixed energy environment, whereas, sedimentary nature tends toward well unsorted is deposited by the steady fluvial energy (high or low) environment. Moreover, the higher mean grain-size with well unsorted (poorly sorted) sediment demonstrates the high energy environment, while, the well unsorted with lower mean grain-size exhibits the low energy environment during deposition. The sedimentary deposits resulted with coarse (positive) skewed indicates the enhanced high energy environment followed by continuous receding energy level. The fine (negative) skewness shows a gradual increase in energy level, which rapidly reduced after achieve the peak level, whereas, the symmetrical skewed reveals a similar trend in the rise and fall of flow regime. The leptokurtic type of sedimentary nature conveys the high energy peak discharge, which becomes mesokurtic to platykurtic nature with reducing discharge and energy level during sediment deposition.

The 3.58 m thick younger fill terrace has been composed of twelve distinct sedimentary layers coupled with diversified sedimentological properties (Table 3.3). Based on the response of the local people it is clear that this fill terrace has been formed after the flood event of 1971, which reveals the fill terrace is 45 years old (as in 2015). The material types of these layers have been composed of different mean grain-size material of sands and silts. Very coarse silt (60 μm) and coarse silt (28 μm) has been found respectively in the 2nd and 3rd layers those were deposited in the low energy and high flow regime as a lag deposit. Such type of depositional environment is supported by the nature of mode (unimodal), sorting (moderately sorted), skewness (symmetrical-coarse) and kurtosis (very leptokurtic-leptokurtic) (Table 3.3). The 6th, 8th, 10th and 11th layers have been resulted with bimodal and well—moderately well sorted sedimentary nature, which indicates that these layers were deposited either in the two or more flood events or by the repetitive fluctuating energy level of a single flood event. The layer-wise depositional environment has been assessed in supports of the nature of skewness and kurtosis. In the 6th layer, sediments were deposited with the effects of moderate energy level which was enhanced up to the high level at the end of the flood event. The 8th layer was deposited initially in the increasing energy level, and it was rapidly reducing after achieved the peak discharge and energy level. The 10th layer was deposited with the fluctuating trend of flow regime dominated by high energy peak discharge. The fluctuating flow regime with reducing discharge and energy level was acting during the deposition of sediments in the 11th layer.

In the excavated profile of older mid-channel bar, twelve distinct sedimentary layers have been characterized by very coarse silt (61 μm)—very coarse sand (1512 μm), although, 1.52–2.75 cm diameter gravels have been observed in 12th layer (Table 3.4). The gravels dominated by very coarse sand (12th layer) was deposited under the very high energy steady flow which was diminishing after achieved the peak regime. The 11th

Table 3.3 Lithostratigraphic characteristics of sedimentary profile of younger fill terrace at Dharmapur

| Layers | Depth (m.bgl) | Material types | Mean grain-size (μm) | Mode | Sorting | Skewness | Kurtosis |
|---------------|---------------------------------|--------------------|-----------------------------------|----------|------------------------|-------------|------------------|
| 1st (top) | 0.00–0.14 | Fine sand | 202 | Unimodal | Well sorted | Coarse | Mesokurtic |
| 2nd | 0.14–0.19 | Very coarse silt | 60 | Unimodal | Moderately sorted | Symmetrical | Very Leptokurtic |
| 3rd | 0.19–0.30 | Fine sand | 214 | Unimodal | Well sorted | Coarse | Leptokurtic |
| 4th | 0.30–0.39 | Coarse silt | 28 | Unimodal | Moderately sorted | Coarse | Leptokurtic |
| 5th | 0.39–0.61 | Fine sand | 206 | Unimodal | Moderately well sorted | Coarse | Mesokurtic |
| 6th | 0.61–0.88 | Fine–medium sand | 248 | Bimodal | Well sorted | Coarse | Mesokurtic |
| 7th | 0.88–1.88 | Medium sand | 265 | Unimodal | Moderately well sorted | Coarse | Platykurtic |
| 8th | 1.88–2.00 | Medium–fine sand | 323 | Bimodal | Moderately well sorted | Fine | Platykurtic |
| 9th | 2.00–2.28 | Medium sand | 460 | Unimodal | Moderately sorted | Symmetrical | Leptokurtic |
| 10th | 2.28–2.63 | Medium–coarse sand | 481 | Bimodal | Well sorted | Symmetrical | Leptokurtic |
| 11th | 2.63–3.43 | Fine–medium sand | 290 | Bimodal | Moderately well sorted | Symmetrical | Platykurtic |
| 12th (bottom) | 3.43–3.58 (up to exposed layer) | Medium sand | 454 | Unimodal | Moderately sorted | Coarse | Platykurtic |

Table 3.4 Lithostratigraphic characteristics of sedimentary profile of older mid-channel bar at Nayabasan

| Layers | Depth (m.bgl) | Material types | Mean grain-size (μm) | Mode | Sorting | Skewness | Kurtosis |
|---------------|---------------------------------|--|-----------------------------------|----------|------------------------|-------------|------------------|
| 1st (top) | 0.00–0.10 | Fine sand | 201 | Unimodal | Moderately well sorted | Symmetrical | Platykurtic |
| 2nd | 0.10–0.21 | Fine–medium sand | 242 | Bimodal | Moderately sorted | Symmetrical | Leptokurtic |
| 3rd | 0.21–0.30 | Fine sand | 178 | Unimodal | Moderately sorted | Coarse | Mesokurtic |
| 4th | 0.30–0.37 | Fine–medium sand | 248 | Bimodal | Moderately sorted | Symmetrical | Mesokurtic |
| 5th | 0.37–0.75 | Medium sand | 405 | Unimodal | Moderately sorted | Symmetrical | Mesokurtic |
| 6th | 0.75–0.87 | Very coarse silt | 61 | Unimodal | Moderately sorted | Coarse | Very Leptokurtic |
| 7th | 0.87–1.05 | Fine sand | 243 | Unimodal | Moderately well sorted | Symmetrical | Platykurtic |
| 8th | 1.05–1.20 | Very fine sand–very coarse silt | 68 | Bimodal | Poorly sorted | Coarse | Leptokurtic |
| 9th | 1.20–1.25 | Coarse sand | 645 | Unimodal | Poorly sorted | Coarse | Mesokurtic |
| 10th | 1.25–1.36 | Medium sand | 451 | Bimodal | Moderately sorted | Fine | Very Leptokurtic |
| 11th | 1.36–1.63 | Fine–medium sand | 245 | Bimodal | Moderately sorted | Symmetrical | Mesokurtic |
| 12th (bottom) | 1.63–1.93 (up to exposed layer) | Very coarse sand with gravels ^a | 1512 | Unimodal | Poorly sorted | Coarse | Leptokurtic |

^aAverage diameter of gravels varies within 1.52–2.75 cm

Table 3.5 Lithostratigraphic characteristics of sedimentary profile of mid-channel bar at Saherbazar

| Layers | Depth (m.bgl) | Material types | Mean grain-size (μm) | Mode | Sorting | Skewness | Kurtosis |
|--------------|---------------------------------|---------------------|-----------------------------------|----------|------------------------|-------------|------------------|
| 1st (top) | 0.00–1.10 | Silt–very fine sand | 31 | Unimodal | Moderately sorted | Coarse | Mesokurtic |
| 2nd | 1.10–2.30 | Medium–fine sand | 245 | Bimodal | Moderately well sorted | Symmetrical | Very Leptokurtic |
| 3rd | 2.30–3.80 | Silt | 15 | Unimodal | Poorly sorted | Fine skewed | Leptokurtic |
| 4th | 3.80–4.75 | Fine sand | 134 | Unimodal | Moderately sorted | Coarse | Leptokurtic |
| 5th | 4.75–5.61 | Silt–clay | 9 | Unimodal | Well sorted | Symmetrical | Mesokurtic |
| 6th (bottom) | 5.61–6.11 (up to exposed layer) | Medium–fine sand | 254 | Unimodal | Moderately well sorted | Coarse | Mesokurtic |

layer was deposited with due effects of reducing energy and flow regime, which again enhanced during the deposition of the 10th layer. Also, the 9th layer might be deposited at the same flood event corresponding to the sedimentation in 10th layer, although, during sediment deposition in the 9th layer, the energy level gradually reduced after achieving the peak level. The river carried silt and very fine sand-size materials during the first flood event (Jana and Paul 2019). Therefore, the 8th layer was deposited in a different flood event in the successive year, which was characterized by the voluminous discharge coupled with the high regime and moderate energy level. The 7th layer was also deposited at the end of this flood event associated with a steady and moderate flow energy environment. The 6th to top (1st) layers were deposited in a different flood year with fluctuating energy and flow regimes.

The sedimentary profile of mid-channel bar (at Saherbazar) has been situated in the wide (910 m) river course, which has swiftly reduced to 350 m at Militaribazar bridge and 250 m at Rajghat bridge only within 2.5 km and 7.5 km downstream section, respectively. In the downstream section (older deltaplain) such kind of channel dimension is responsible for clay–medium sand types of material deposition in the six diversified sedimentary layers within 6.11 m elevated bar (compared to local river bed) (Table 3.5). The medium–fine sand (254 μm) was deposited at the bottom layer under the moderately steady energy condition which was reduced at the end of the flood event. The silt–clay type materials in the 4th layer (0.86 m thick) were deposited with voluminous sediment loaded low energy steady flow energy environment. In the 4th layer, fine sands were deposited in a separate flood event characterized by moderate energy steady enhancing followed by continuous receding energy environment. The silt was deposited in the 3rd layer under the dominance of low energy and firmly reducing flow regime. The medium–fine sand-size materials (in 2nd layer) were deposited in two different flood events under moderate–high energy fluctuating flow regimes. The top layer (silt–very fine sand) was

formed with due effects from the mixed energy fluctuating flow regime of a single flood event. The top layer was deposited during 1978 and after that flood level was unable to inundate the stable platform of the bar. About 1.0–1.5 m diameter tree logs have been observed over the bar surface, which assists to predict the age of the bar. Local people are also confirmed that the bar has been formed about 25 years ago (as in 2015).

3.5 Conclusion

The present study area of the middle-lower and deltaic courses of the Subarnarekha river represent a significant sediment sink. A large amount of sand size sediments is derived from the upper catchment area dominated by weathered granites and gneissic terrain of the Chotanagpur plateau. The depositional environments of the study area represent high fluvial influx in the three sections of the channel reaches from Jamsola to Ragra, Ragra to Dantan, and Dantan to Rajghat. However, the assemblages of landforms, geometry of the channel reach and sediment characteristics of the downstream section indicate the role of concomitant sea level fluctuations in the modification of sedimentary depositional environment. The plan shape geomorphology, properties of channel geometry, sediment texture and stratigraphic sections of the river valley alluviums, morphology of the mid-channel bars, and palaeo-shorelines of the deltaic section reveal the presence of very distinct depositional sub-environments along the present course of the Subarnarekha river from Jamsola to Chaumukh. The study also highlights the role of energy level fluctuations of the river flow since the Late Pleistocene to Early Holocene period, and continuous adjustment of the channel course since Early–Late Holocene period with the base level changes resulted from marine transgression, regression and stillstand phases. The presence of valley cuts, fluvial and marine terraces also indicate the role of neotectonics in the modifications of bank margin environment of the river valley.

Acknowledgements The authors are grateful to the United States Geological Survey (USGS) for making available the satellite images, and also thankful to the Government of India for making available the Geological Quadrangle Map on Open Government Data (OGD) platform free of charge. The corresponding author would like to acknowledge the University Grants Commission, New Delhi, India, for financial support as Junior Research Fellowship [Award Letter No.: F.15-6(DEC.2014)/2015 (NET), UGC Ref. No. 3070/(NET-DEC.2014)] to carry out the research work presented in this paper.

References

- Abrahams AD (1984) Channel networks: a geomorphological perspective. *Water Resour Res* 20(2):161–188
- Ashworth PJ, Best JL, Roden JE, Bristow CS, Klaassen GJ (2000) Morphological evolution and dynamics of a large, sand braid-bar, Jamuna River, Bangladesh. *Sedimentology*. 47(3):533–555
- Banerjee M, Sen PK (1987) Palaeobiology in understanding the changes of sea-level and coastline in Bengal Basin during Holocene Period. *Indian J Earth Sci* 14:307–320
- Bannerjee M, Sen PK (1988) Paleobiology and environment of deposition of Holocene sediments of the Bengal Basin, India. In: *Paleoenvironment of East Asia from the mid-Tertiary: Proceedings of the Second Conference*. Hong Kong Centre of Asian Studies, University of Hong Kong, 703–731
- Bentham PA, Talling PJ, Burbank DW (1993) Braided stream and flood-plain deposition in a rapidly aggrading basin: the Escanilla Formation, Spanish Pyrenees. In: Best JL, Bristow CS (eds) *Braided Rivers*. *Geol Soc Spec Publ* 75(1):177–94. <https://doi.org/10.1144/GSL.SP.1993.075.01.11>
- Best J (2019) Anthropogenic stresses on the world's big rivers. *Nat Geosci* 12(1):7–21
- Beuchle R, Grecchi RC, Shimabukuro YE, Seliger R, Eva HD, Sano E, Achard F (2015) Land cover changes in the Brazilian Cerrado and Caatinga biomes from 1990 to 2010 based on a systematic remote sensing sampling approach. *Appl Geogr* 58:116–127
- Bhattacharya A, Misra AK (1984) Geological remote sensing in parts of Subarnarekha—Baitarani basin, Eastern India. *J Indian Soc Remote* 12(1):19–28
- Bishop MP, James LA, Shroder JF Jr, Walsh SJ (2012) Geospatial technologies and digital geomorphological mapping: concepts, issues and research. *Geomorphology* 137(1):5–26
- Bisson PA, Montgomery DR, Buffington JM (2017) Valley segments, stream reaches, and channel units. In: Hauer FR, Lamberti GA (eds) *Methods in Stream Ecology*. Elsevier, San Francisco, pp 21–47
- Blott SJ, Pye K (2001) GRADISTAT: a grain size distribution and statistics package for the analysis of unconsolidated sediments. *Earth Surf Proc Land* 26(11):1237–1248
- Corenblit D, Tabacchi E, Steiger J, Gurnell AM (2007) Reciprocal interactions and adjustments between fluvial landforms and vegetation dynamics in river corridors: a review of complementary approaches. *Earth-Sci Rev* 84(1–2):56–86
- Dandapat K, Panda GK (2013) Drainage and floods in the Subarnarekha Basin in Paschim Medinipur, West Bengal, India—a study in applied geomorphology. *Int J Sci Res* 4:791–797
- Foody GM, Campbell NA, Trodd NM, Wood TF (1992) Derivation and applications of probabilistic measures of class membership from the maximum-likelihood classification. *Photogramm Eng Rem S* 58(9):1335–1341
- Fryirs KA, Brierley GJ (2012) *Geomorphologic analysis of river systems: an approach to reading the landscape*. John Wiley & Sons
- Geological Survey of India (1998) *Geological Quadrangle Map*, Geological Survey of India, Government of India, available on https://www.gsi.gov.in/webcenter/portal/OCBIS/pageMAPS/pageMapsSeries?_adf.ctrl-state=wd51swrgt_5&_afLoop=27454911959312140 ↓, retrieved on 6th December, 2015.
- Ghosh S, Guchhait SK (2020) *Laterites of the Bengal Basin: Characterization*. Springer, Geochronology and Evolution
- Gilvear DJ (1999) Fluvial geomorphology and river engineering: future roles utilizing a fluvial hydrosystems framework. *Geomorphology* 31(1–4):229–245
- Goswami AB (1997) A morphostratigraphic hydrologic and hydrochemical appraisal. Reprint of 8th National symposium on Hydrology, Jadavpur University, Calcutta, Medinipur coastal belt, WB, pp 30–40.
- Goswami AB (1999) Quaternary mapping concept constraints, aims and approaches with special reference to Bengal Basin. Workshop manual on coastal quaternary. Bengal Basin, Bose inst., Calcutta, 4–9(1):1–20.
- Guha S, Patel PP (2017) Evidence of topographic disequilibrium in the Subarnarekha River Basin, India: A digital elevation model based analysis. *J Earth Sys Sci* 126(7):106
- Ilahi RA, Dutta S (2016) Quantification and Mapping of Morphometric Parameters of Subarnarekha River Basin in Eastern India using Geo-Spatial Techniques. *Indian Cartog* 16:184–197
- Islam A, Guchhait SK (2017) Analysing the influence of Farakka Barrage Project on channel dynamics and meander geometry of Bhagirathi river of West Bengal, India. *Arab J Geosci* 10(11):245
- Jana S (2019) An automated approach in estimation and prediction of riverbank shifting for flood-prone middle-lower course of the Subarnarekha River. *Int J River Basin Manag*, India. <https://doi.org/10.1080/15715124.2019.1695259>
- Jana S, Paul AK (2014) Morphodynamics of the meandering river: A study along the Subarnarekha river of

- Gopiballavpur section, West Bengal, India. *Int J Geol Earth Env Sci* 4(3):219–230
- Jana S, Paul AK (2018) Genetical Classification of Deltaic and Non Deltaic Sequences of Landforms of Subarnarekha Middle Course and Lower Course Sections in Odisha and Parts of West Bengal with Application of Geospatial Technology. *J Coast Sci* 5 (1):16–26
- Jana S, Paul AK (2019) Assessment of morphogenetic sedimentary depositional environments of different morphological surfaces of middle-lower and deltaic courses of Subarnarekha River. *J Coast Sci* 6(1):1–11
- Jana S, Paul AK (2020) Chronological evolution of the channel functional units in association with palaeo-hydrogeomorphological environment in the ancient delta fan of Subarnarekha basin. *India. Environ Earth Sci* 9:331. <https://doi.org/10.1007/s12665-020-09093-1>
- Jana S, Paul AK, Islam SM (2014) Morphodynamics of Barrier Spits and Tidal Inlets of Subarnarekha Delta: a study at Talsari-Subarnapur spit, Odisha, India. *Indian J Geo Env* 13:23–32
- Jia K, Wei X, Gu X, Yao Y, Xie X, Li B (2014) Land cover classification using Landsat 8 operational land imager data in Beijing, China. *Geocarto Int* 29 (8):941–951
- Jia K, Wu B, Tian Y, Zeng Y, Li Q (2011) Vegetation classification method with biochemical composition estimated from remote sensing data. *Int J Remote Sens* 32(24):9307–9325
- Khan A, Rao LA, Yunus AP, Govil H (2018) Characterization of channel planform features and sinuosity indices in parts of Yamuna River flood plain using remote sensing and GIS techniques. *Arab J Geosci* 11 (17):525
- Leopold LB, Wolman MG, Miller JP (1992) *Fluvial processes in geomorphology*, 2nd edn. Dover Publishers, New York, p 522
- Mokarrama M, Hojati M (2018) Landform classification using a sub-pixel spatial attraction model to increase spatial resolution of digital elevation model (DEM). *Egypt J Remote Sens Space Sci* 21(1):111–120
- Niyogi D (1975) Quaternary Geology of the coastal plain of West Bengal and Orissa. *Indian J Earth Sci* 2 (1):51–61
- Pal M, Foody GM (2012) Evaluation of SVM, RVM and SMLR for accurate image classification with limited ground data. *IEEE J Sel Topics Appl Earth Obs Remote Sens* 5(5):1344–1355
- Patel A, Katiyar SK, Prasad V (2016) Performances evaluation of different open source DEM using Differential Global Positioning System (DGPS). *Egypt J Remote Sens Space Sci* 19(1):7–16
- Paul AK (2002) *Coastal Geomorphology and Environment: Sundarban Coastal Plain, Kanthi Coastal Plain*. ACB publications, Kolkata, Subarnarekha Delta Plain
- Paul AK, Kamila A (2016) Coastal Mud Banks of Subarnarekha Delta with Special Reference to Degradation and Accretion under Physical Processes. *Indian Cartog* 16:13–24
- Pavlis NK, Holmes SA, Kenyon SC, Factor JK (2012) The development and evaluation of the Earth Gravitational Model 2008 (EGM2008). *J Geophys Res-Sol Ea* 117:B044406. <https://doi.org/10.1029/2011JB008916>
- Poff NL, Allan JD, Bain MB, Karr JR, Prestegard KL, Richter BD, Sparks RE, Stromberg JC (1997) The natural flow regime. *Bioscience* 47(11):769–784
- Roy S, Sahu AS (2018) Road-stream crossing an in-stream intervention to alter channel morphology of headwater streams: case study. *Int J River Basin Manag* 16(1):1–9
- Samanta RK, Bhunia GS, Shit PK, Pourghasemi HR (2018) Flood susceptibility mapping using geospatial frequency ratio technique: a case study of Subarnarekha River Basin, India. *Model Earth Syst Environ* 4 (1):395–408
- Sarma JN (2005) Fluvial process and morphology of the Brahmaputra River in Assam, India. *Geomorphology*. 70(3–4):226–256
- Sofia G (2020) Combining geomorphometry, feature extraction techniques and Earth-surface processes research: The way forward. *Geomorphology*. <https://doi.org/10.1016/j.geomorph.2020.107055>
- Ventra D, Clarke LE (2018) Geology and geomorphology of alluvial and fluvial fans: current progress and research perspectives. *Geol Soc Spec Publ* 440(1):1–21
- Wharton G (1995) The channel-geometry method: guidelines and applications. *Earth Surf Proc Land* 20 (7):649–660
- Williams GP (1986) River meanders and channel size. *J Hydrol* 88(1–2):147–164
- Wu B, Xia J, Fu X, Zhang Y, Wang G (2008) Effect of altered flow regime on bankfull area of the Lower Yellow River, China. *Earth Surf Proc Land* 33 (10):1585–1601